JOURNAL OF VIROLOGY, Nov. 2002, p. 11530–11540 Vol. 76, No. 22
0022-538X/02/$04.00+0 DOI: 10.1128/JVI.76.22.11530–11540.2002
Copyright © 2002, American Society for Microbiology. All Rights Reserved.

Cell-Type-Specific Characteristics Modulate the Transduction Efficiency of Adeno-Associated Virus Type 2 and Restrain Infection of Endothelial Cells

Katri Pajusola,[1]* Marcin Gruchala,[2] Hana Joch,[3] Thomas F. Lüscher,[3] Seppo Ylä-Herttuala,[2] and Hansruedi Büeler[1]

Institute of Molecular Biology, University of Zurich, 8057 Zurich,[1] and Department of Cardiology and Cardiovascular Research, University Hospital, 8091 Zürich,[3] Switzerland, and A. I. Virtanen Institute, University of Kuopio, 70210 Kuopio, Finland[2]

Received 14 June 2002/Accepted 7 August 2002

Adeno-associated viruses (AAVs) are promising vectors for various gene therapy applications due to their long-lasting transgene expression and wide spectrum of target cells. Recently, however, it has become apparent that there are considerable differences in the efficiencies of transduction of different cell types by AAVs. Here, we analyzed the efficiencies of transduction and the transport mechanisms of AAV type 2 (AAV-2) in different cell types, emphasizing endothelial cells. Expression analyses in both cultured cells and the rabbit carotid artery assay showed a remarkably low level of endothelial cell transduction in comparison to the highly permissive cell types. The study of the endosomal pathways of AAV-2 with fluorescently labeled virus showed clear targeting of the Golgi area in permissive cell lines, but this phenomenon was absent in the endothelial cell line EAhy-926. On the other hand, the response to the block of endosomal acidification by bafilomycin A1 also showed differences among the permissive cell types. We also analyzed the effect of proteasome inhibitors on endothelial cells, but their impact on the primary cells and in vivo was not significant. On the contrary, analysis of the expression pattern of heparan sulfate proteoglycans (HSPGs), the primary receptors of AAV-2, revealed massive deposits of HSPG in the extracellular matrix of endothelial cells. The matrix-associated receptors may therefore compete for virus binding and reduce transduction in endothelial cells. Accordingly, in endothelial cells detached from their matrix, AAV-2 transduction was significantly increased. Altogether, these results point to a more complex cell-type-specific mode of transduction of AAV-2 than previously appreciated.

Adeno-associated viruses (AAVs) belong to the human parvoviruses and within this family to the genus *Dependovirus* because they require a helper virus, for example, adenovirus, to go through a productive life cycle (3). AAVs have in recent years been under intense research due to their potential as promising gene transfer vehicles: AAV is not known to be pathogenic and causes only a subtle immune response in vivo, AAV-mediated gene transfer results in very long-lasting gene expression, and AAV is able to infect a variety of cell types in either the proliferating or quiescent state (20, 29). Different serotypes of AAV have been shown to have varying preferences in their target cell type of choice, and this can be utilized in the potential gene therapy applications (5, 15). Of the six different AAV serotypes, the best characterized so far is serotype 2 (AAV-2), and this serotype was the focus of the present study. Although AAV-2 is known to be able to infect many different cell types, recent data have shown various cellular factors that influence the efficiency of transduction and have led to the identification of cell types which are highly or poorly permissive for AAV-2 transduction. The primary attachment receptor of AAV-2 is heparan sulfate proteoglycan (HSPG) (32). Although this highly heterogeneous gene family is widely expressed on many cell types, there are cells that lack HSPG expression, and such cells have been shown to be resistant to AAV-2 infection (32). Besides the primary receptor, AAV-2 needs to utilize a coreceptor for cell internalization, and so far there are two receptors identified for this purpose: αV-β5 integrin and fibroblast growth factor receptor-1 (24, 31). All the receptors for AAV-2 are molecules which are commonly expressed on endothelial cells (30, 34), the cell type we focused on here, and therefore endothelial cells should not have a limitation for AAV-2 transduction in this respect. Data concerning AAV-2 cytoplasmic transport have been largely obtained by studies performed with HeLa cells, a cell line which is highly permissive for AAV-2 transduction (2, 8). These studies have shown that AAV-2 is internalized via receptor-mediated endocytosis and thereafter travels in the endosomal compartment up to the late endosomes. Before entering the nucleus, AAV-2 may be released into the cytoplasm. Due to its small size, it has been suggested that AAV can traverse the nuclear pores without prior uncoating (17). The requirement for late-endosome entry has been studied using bafilomycin A1, which efficiently inhibits endosomal acidification and thereby also inhibits endosomal maturation (2, 7, 16). Another factor that was also recently shown to limit AAV-2 transduction in some cell types is proteasome activity, which has been studied by using various proteasome inhibitors (7, 9). In this study, we wanted to explore AAV-2 transduction of endothe-

* Corresponding author. Mailing address: Institute of Molecular Biology, University of Zurich, Winterthurerstrasse 190, 8057 Zurich, Switzerland. Phone: 41-1-635 3181. Fax. 41-1-635 6830. E-mail: pajusola@molbio.unizh.ch.

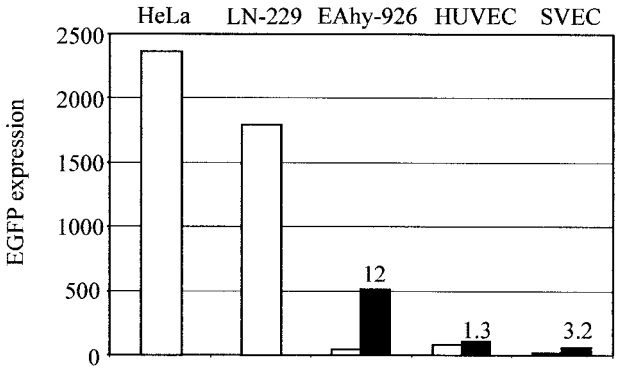

FIG. 1. AAV-2 transduction efficiency measured by FACS analysis of EGFP expression. Cells were infected with AAV2-CMV-EGFP-WPRE at an MOI of 200, and EGFP expression was measured 48 (cell lines) or 72 h (primary cells) after infection. The arbitrary value of the EGFP expression was calculated by multiplying the percentage of positive cells by the intensity of the expression. An experiment representative of several repeats is shown. The open bars represent untreated cells, and the solid bars (EAhy-926 cells, HUVEC, and SVEC) represent the expression after MG-132 treatment. The values above the bars indicate the increase (*n*-fold) of expression after MG-132 treatment.

lial cells, because these cells are an interesting target for several gene therapy applications, for example, in the context of cancer or cardiovascular diseases. Our findings reveal interesting new aspects of AAV-2 transduction pathways which add to the complexity of the cell-type-specific transduction mechanisms.

MATERIALS AND METHODS

AAV-2 production. AAV2-CMV-EGFP-WPRE and AAV2-CMV-EGFP were produced in 293T cells by double plasmid transfection with calcium phosphate coprecipitation. The psub-CMV-EGFP-WPRE or psub-CMV-EGFP (23) and pDG (13) plasmids were used for the transfection. The virus preparations were purified by iodixanol gradient ultracentrifugation and heparin-Sepharose high-performance liquid chromatography, as described previously (41). The physical titers were determined by slot blot hybridization.

Antibodies. A20 monoclonal antibody (MAb), which recognizes the intact AAV-2 particle, was purchased from Progen Immunodiagnostika, Heidelberg, Germany, and used at a 1:2 dilution. The rabbit anti-galactosyltransferase antibody, a kind gift of Eric Berger, was used at a 1:2,000 dilution. Anti-heparan sulfate (HS) MAb 10E4-fluorescein isothiocyanate (FITC) conjugate was purchased from Seikagaku Corp., Tokyo, Japan (used at a 1:12.5 dilution). Rat anti-mouse CD31 was purchased from PharMingen (used at a 1:200 dilution). Donkey anti-mouse–FITC (Jackson ImmunoResearch Inc.), rabbit anti-mouse–Alexa488, goat anti-rat–Alexa546, and goat anti-rabbit–Alexa594 (Molecular Probes) secondary antibodies were used at 1:100 to 1:300 dilutions.

Cell culture. 293T, HeLa, LN-229 (a kind gift of Isabelle Desbaillets, University of Zürich) (36), and EAhy-926 (10) cells were cultured in Dulbecco's modified Eagle's medium (DMEM; Gibco)–10% fetal calf serum (FCS). Human umbilical vein endothelial cells (HUVEC) and human saphenous vein endothelial cells (SVEC) were dissected and cultured as described earlier (39), and cells from the second and third passages were used for the experiments.

AAV-2 expression assay. Cells were seeded on six-well culture dishes so that they became subconfluent overnight (4×10^5 to 6×10^5/well). Primary endothelial cells were seeded on fibronectin (Gibco)-coated wells and cultivated for 2 days before the AAV-2 infections. The AAV2-CMV-EGFP-WPRE stock was diluted in DMEM–2% FCS or EGM2 (Bio-Whittaker)–2% FCS to the required multiplicity of infection (MOI; physical particles per cell), the cells were washed once with the low-FCS medium, and the virus dilutions were applied to the cells. Different cell types were tested simultaneously to allow comparison of the cell-type-specific differences. Infections were carried out for 2 h, or 4 h in the case of primary endothelial cells, after which the cells were changed to 10% FCS medium and incubation was continued for 46 or 68 h. For the infection of human primary endothelial cells in suspension, the cells were detached with 20 mM EDTA, after which infection was carried out in suspension for 1 h before the cells were replated on fibronectin-coated culture dishes. When the effects of bafilomycin A1 (20 nM; Sigma) and MG-132 (10 μM; Calbiochem) on the transduction were tested, the drugs were present during the incubation with virus, after which the cells were washed and incubation was continued.

Texas Red labeling of AAV-2. AAV2-Tie-EGFP-WPRE was produced and purified as described above. The plasmid construct of AAV2-Tie-EGFP-WPRE was prepared by replacing the cyomegalovirus (CMV) promoter fragment in AAV2-CMV-EGFP-WPRE by the Tie promoter fragment (19), a kind gift of Kari Alitalo, University of Helsinki). Particles (2×10^{12}) were labeled with Texas Red (TxR) (a kind gift of Urs Greber) as described previously (12) with some modifications. The labeled preparation was purified from the free label by extensive dialysis. As the last step, TxR-AAV2 was dialyzed in DMEM and stored in aliquots at −80°C.

Immunofluorescence experiments. Cells were seeded on Alcian Blue (1% solution; Sigma)- or Alcian Blue-fibronectin-coated glass coverslips and cultivated overnight. Incubations were done with TxR-AAV2 as specified in Results below. After the incubations, the cells on the coverslips were washed in phosphate-buffered saline (PBS) and fixed with 4% paraformaldehyde (Sigma-Aldrich) for 30 min. The cells were permeabilized with 0.1% Triton X-100 for 10 min and blocked in 10% FCS for 30 to 60 min. A20 antibody incubation was carried out at 4°C overnight. The other primary antibodies were incubated for 1 h at room temperature. The secondary antibodies were incubated for 45 min at room temperature. The coverslips were mounted with FluorSave (Calbiochem) for microscopy.

FACS analysis. Cells were dissociated from the culture dish either by trypsinization (enhanced green fluorescent protein [EGFP] expression) or with 20 mM EDTA (anti-HS-FITC staining). EGFP-expressing cells were suspended in PBS–1 mM $MgCl_2$–1 mM $CaCl_2$–2% FCS and measured in the Beckman Coulter EPICS XL flow cytometer. The FACS control samples were treated with the same drug concentrations as the AAV-2-infected samples to exclude drug-induced autofluorescence. Anti-HS-FITC antibody was incubated with the cells in PBS on ice for 1 h, after which the cells were washed and measured. Cells dissociated and incubated under the same conditions without the antibody were used as controls.

Animal experiments. Male New Zealand White rabbits ($n = 9$; 2.2 to 3.0 kg) were anesthetized subcutaneously (s.c.) with fentanyl-fluonisone (Hypnorm; Janssen Pharmaceutica) at 0.2 ml/kg of body weight and s.c. with midazolam (Dormicum; Roche) at 1.5 mg/kg. All animals received anticholinergic glycopyrronium (Robinul; John Wyeth and Brother Ltd.) s.c. at 0.05 mg/kg and cefuroxim (Zinacef; GlaxoWellcome) s.c. at 125 mg/kg before surgery (40). The left carotid artery was exposed by a midline neck incision; vascular spasm was averted with topical lidocaine 1% (Lidocain; Orion), and enoxaparin (Klexane; Rhone-Poulenec Rorer) at 1 mg/kg was administered intravenously. For gene transfer, a 1.5- to 2.5-cm segment of the carotid artery was isolated between atraumatic vascular clamps, and two 24-gauge Neoflon cannulas (Becton Dickinson) were introduced into the lumen through proximal and distal arteriotomy. The lumen of the vessel was cleared of blood by gentle flushing with 0.9% saline, and approximately 100 μl of an AAV2-CMV-EGFP-WPRE vector with or without 40 μM MG-132 or the same volume of 0.9% saline was instilled into the vessel lumen and allowed to dwell in situ for 20 min. After the incubation period, the vessel lumen was flushed with 0.9% saline, the arteriotomies were repaired using 10/0 Ethilon sutures (Johnson & Johnson), and blood flow was restored by removing the clamps. Three rabbits were studied in each study group (AAV2-CMV-EGFP-WPRE with MG-132, AAV2-CMV-EGFP-WPRE without MG-132, and 0.9% saline). The animals were sacrificed 21 days after gene transfer. The rabbits were anesthetized and heparinized (600 IU intravenously), and both the left (infected) and right (intact) carotid arteries were dissected free. The animals were killed by intravenous infusion of magnesium sulfate solution, and the vessels were excised and washed in 0.9% saline. The sites of arterial clamping and cannulation were not harvested. All animal procedures were approved by the Animal Care and Use Committee, University of Kuopio, Kuopio, Finland.

Histology. Each carotid specimen was divided into two equal parts. The proximal part was fixed in 4% paraformaldehyde–0.15 M sodium phosphate buffer for 15 min, rinsed with 0.15 M sodium phosphate buffer (pH 7.2), and then embedded in OCT compound (Sakura) and stored at −70°C. The distal part was immersion fixed in 4% paraformaldehyde–15% sucrose (pH 7.4) for 4 h, rinsed in 15% sucrose (pH 7.4) overnight, and embedded in paraffin (40).

Evaluation of EGFP gene expression. Twenty 10-μm-thick frozen carotid artery sections were cut at intervals of at least 50 μm and evaluated for intensity and distribution of EGFP gene expression using fluorescence microscopy with an AX70 microscope (Olympus Optical). The gene transfer efficacy was scored separately in the endothelium intima, media, and adventitia using the following

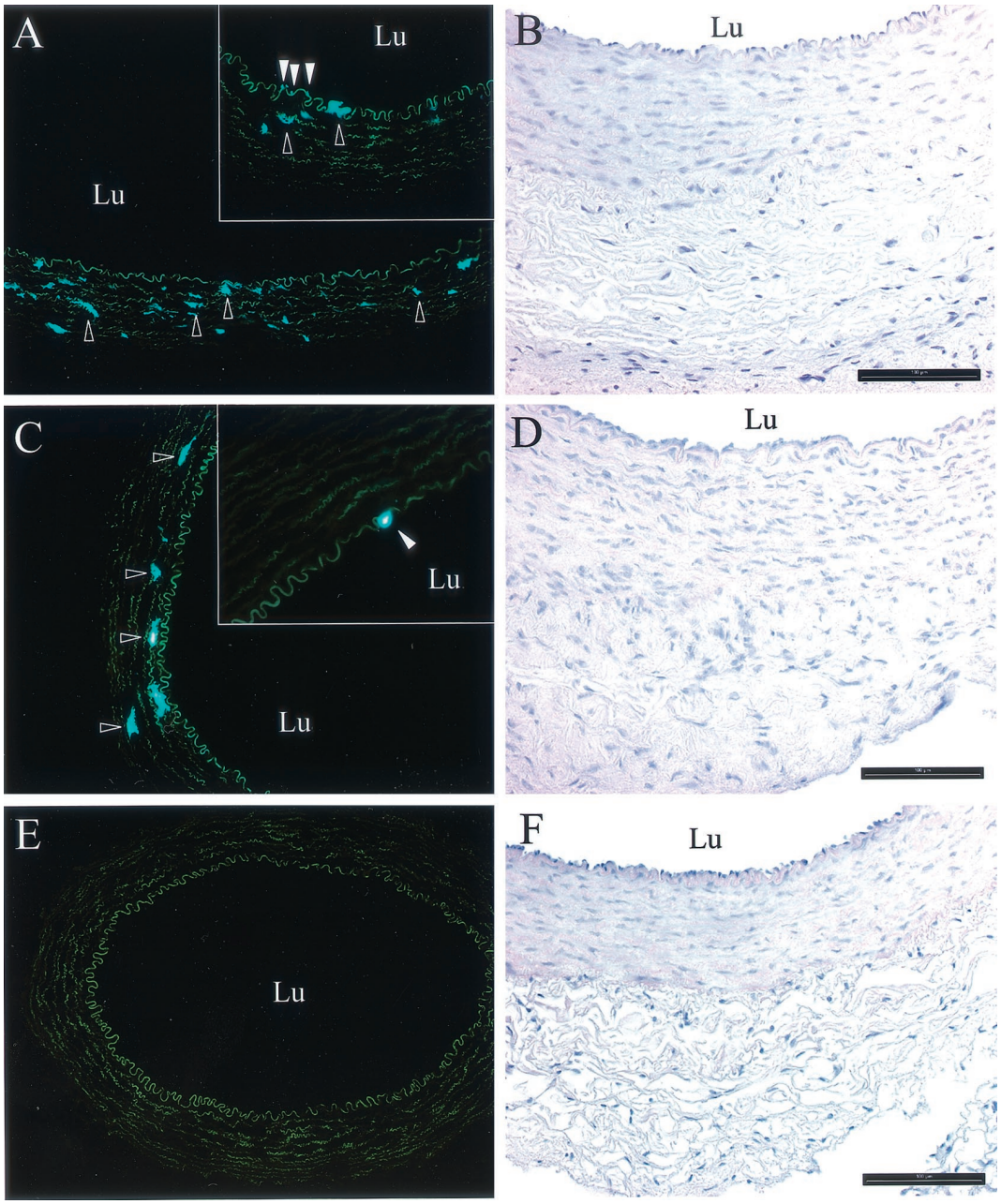

FIG. 2. AAV2-CMV-EGFP-WPRE expression in the rabbit carotid artery assay. Representative micrographs of histological localization of EGFP-positive cells (fluorescent microscopy; dark-field images) and morphology of rabbit carotid arteries (HE staining) 21 days after AAV-2 gene transfer are shown. (A) AAV2-CMV-EGFP-WPRE. The outlined arrowheads indicate examples of EGFP-positive vascular SMCs in medium. In the inset, the open arrowheads indicate EGFP-positive endothelial cells, and the outlined arrowheads indicate examples of EGFP-positive vascular SMCs in medium. (B) HE staining. (C) AAV2-CMV-EGFP-WPRE and MG-132. The outlined arrowheads indicate examples of EGFP-positive vascular SMCs in medium. In the inset, the open arrowhead indicates an EGFP-positive endothelial cell. (D) HE staining. (E) Mock-transfected artery (0.9% saline). (F) HE staining. Fluorescence microscopy original magnification, 10×; insets, 20×; HE staining original magnification, 20×. Lu, lumen of the artery. Bars = 100 μm.

semiquantitative scale: −, no EGFP expression; +, weak expression (occasional EGFP-positive cells present in less than half of the analyzed cross sections); ++, moderate expression (more than two EGFP-positive cells present in more than half of the analyzed cross sections; and +++, high expression (multifocal EGFP presence in all analyzed cross sections).

Evaluation of vascular morphology and local inflammation after gene transfer. The morphology and presence of inflammation after AAV gene transfer and mock transfection were determined using hematoxylin and eosin (HE) staining and immunostaining for endothelial cells (MAb CD31 [DAKO]; dilution, 1:50), smooth muscle cells (SMCs) (MAb HHF-35 [Enzo Diagnostics]; dilution, 1:50), and macrophages (MAb RAM11 [DAKO]; dilution 1:100).

RESULTS

Transduction efficiency of AAV-2 in endothelial cells is low. The transducibility of endothelial cells by AAV-2 was studied in the EAhy-926 cell line, as well as in primary HUVEC and

TABLE 1. EGFP gene expression 21 days after AAV-2 gene transfer to rabbit carotid arteries

Treatment	EGFP expression[a]		
	Intima	Media	Adventitia
AAV2-CMV-EGFP-WPRE	+	+++	−
AAV2-CMV-EGFP-WPRE	+	+++	−
AAV2-CMV-EGFP-WPRE	+	++	−
AAV2-CMV-EGFP-WPRE + MG132	+	+++	−
AAV2-CMV-EGFP-WPRE + MG132	+	++	−
AAV2-CMV-EGFP-WPRE + MG132	−	++	−

[a] + and − reflect the intensity of EGFP expression as follows: −, no EGFP expression; +, weak expression (occasional EGFP-positive cells present in less than half of the analyzed cross sections); ++, moderate expression (more than two EGFP-positive cells present in more than half of the analyzed cross sections); +++, high expression (multifocal EGFP presence in all analyzed cross sections as judged by fluorescence microscopy). Three animals from each group were analyzed.

SVEC. For comparison, we used the human glioma cell line LN-229 and the human cervical carcinoma cell line HeLa, known to be highly permissive for AAV-2 transduction. All cell types were infected at an MOI of 200 (particles/cell) of AAV2-CMV-EGFP-WPRE, and the transduction efficiency, measured as EGFP expression, was analyzed 48 or 72 h later by flow cytometry. The analysis showed that all endothelial cells were transduced with a substantially lower efficiency than the reference cell lines; the difference between EAhy-926 and HeLa cells and that between EAhy-926 and LN-229 cells were 55- and 42-fold, respectively (Fig. 1). The transduction of the primary endothelial cells was more variable but in the same range as that with EAhy-926. Interestingly, the transduction efficiency in the primary endothelial cells could be increased three- to fourfold by a longer vector exposure, up to overnight (data not shown), a phenomenon also demonstrated by others (33). The transducibility of the cell lines, however, did not differ depending on either the length of the vector exposure or increases in the postinfection culture time. The possibility of differential promoter strengths in the cell types studied was excluded by transfection assays, which showed equally strong activities of the CMV promoter in all cells (data not shown).

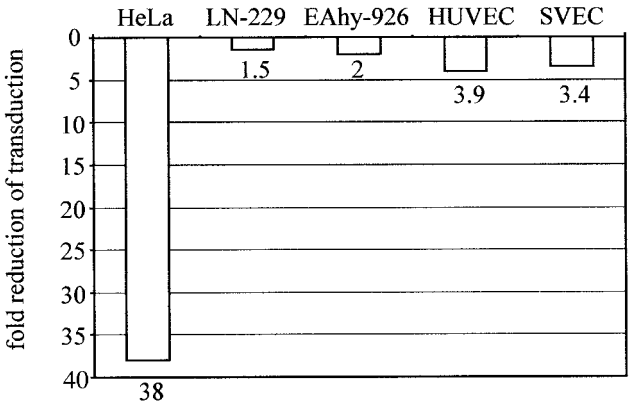

FIG. 3. Influence of bafilomycin A1 on AAV-2 transduction efficiency. Cells were infected in the presence or absence of bafilomycin A1 (20 nM), and EGFP expression was analyzed as described in the legend to Fig. 1. The values under the bars indicate the decrease (*n*-fold) in EGFP expression compared to the untreated infections.

AAV-2 transduction in the in vivo vascular model. We wanted to analyze the AAV-2 transduction efficiency of endothelial cells in vivo, and for this purpose we used the rabbit carotid artery assay. AAV2-CMV-EGFP-WPRE was applied in the lumen of the arteries, and the vessels were analyzed 3 weeks later as described in Materials and Methods. No or very weak EGFP expression was detected in the endothelial cells of the intima, but part of the medial SMCs expressed moderate to high levels of the transgene (Fig. 2 and Table 1). No EGFP expression was present in the adventitia, and the saline-treated control vessels also did not show any EGFP fluorescence. As a comparison, we tested the ability of the Tie promoter (19) to drive transgene expression in this assay, but it was shown to be inefficient and not endothelial cell specific (data not shown). The morphological analysis of the AAV-2-treated arteries showed that all of the harvested arteries were patent and lacked evidence of damaged vessel architecture. The endothelial cell layer had remained intact, and there were no signs of significant inflammatory cell infiltration in either AAV-2- or mock-transfected arteries.

Influence of proteasome inhibitors on AAV-2 transduction. Recently, proteasome activity has been shown to act as a limiting factor for AAV-2 transduction in certain less permissive cell types, such as primary fibroblasts and Hep-G2 cells (7, 9). Here, we studied the effect of inhibition of the proteasome by MG-132 both on cultured endothelial cells and in vivo. In the case of EAhy-926 cells, MG-132 drastically improved transduction, as shown by a 12-fold increase in EGFP expression (Fig. 1). In the permissive HeLa and LN-229 cells also, the transduction was further enhanced fourfold by MG-132. In the primary endothelial cells, however, as well as in the rabbit carotid artery assay, proteasome inhibition had only a modest, if any, effect on transduction (Fig. 1 and 2 and Table 1). In all cases where MG-132 enhanced transduction, it especially increased the intensity of the transgene expression. This could point to the nuclear proteasomes already acting on the virus population in the nucleus (26). Thus, the lack of an effect of proteasome inhibition would indicate a block on an earlier phase of the AAV-2 transduction pathway. Involvement of the lysosomal proteases in AAV-2 transduction was excluded by experiments in the presence of the broad-range lysosomal protease inhibitor E64, which had no effect on transduction efficiency (not shown).

AAV-2 uses alternative endosomal pathways for its cytoplasmic routing. After internalization, AAV travels through the endosomal pathway toward the nucleus, and it has been shown that for efficient transduction it has to enter the late, acidic endosomes before being released to the perinuclear space (2, 7). This has been studied, for example, by infecting cells with AAV-2 in the presence of bafilomycin A1, which is a specific inhibitor of the vacuolar proton pump and thereby inhibits endosomal acidification. In bafilomycin A1-treated HeLa or 293 cells, AAV-2 transduction has been shown to be considerably impaired (2, 7). We wanted to study the AAV-2 endosomal pathway in endothelial and glioma cells to determine whether the observed differences in transduction efficiencies can be explained by a different endosomal-routing behavior of AAV-2. HUVEC, SVEC, and EAhy-926, LN-229, and HeLa

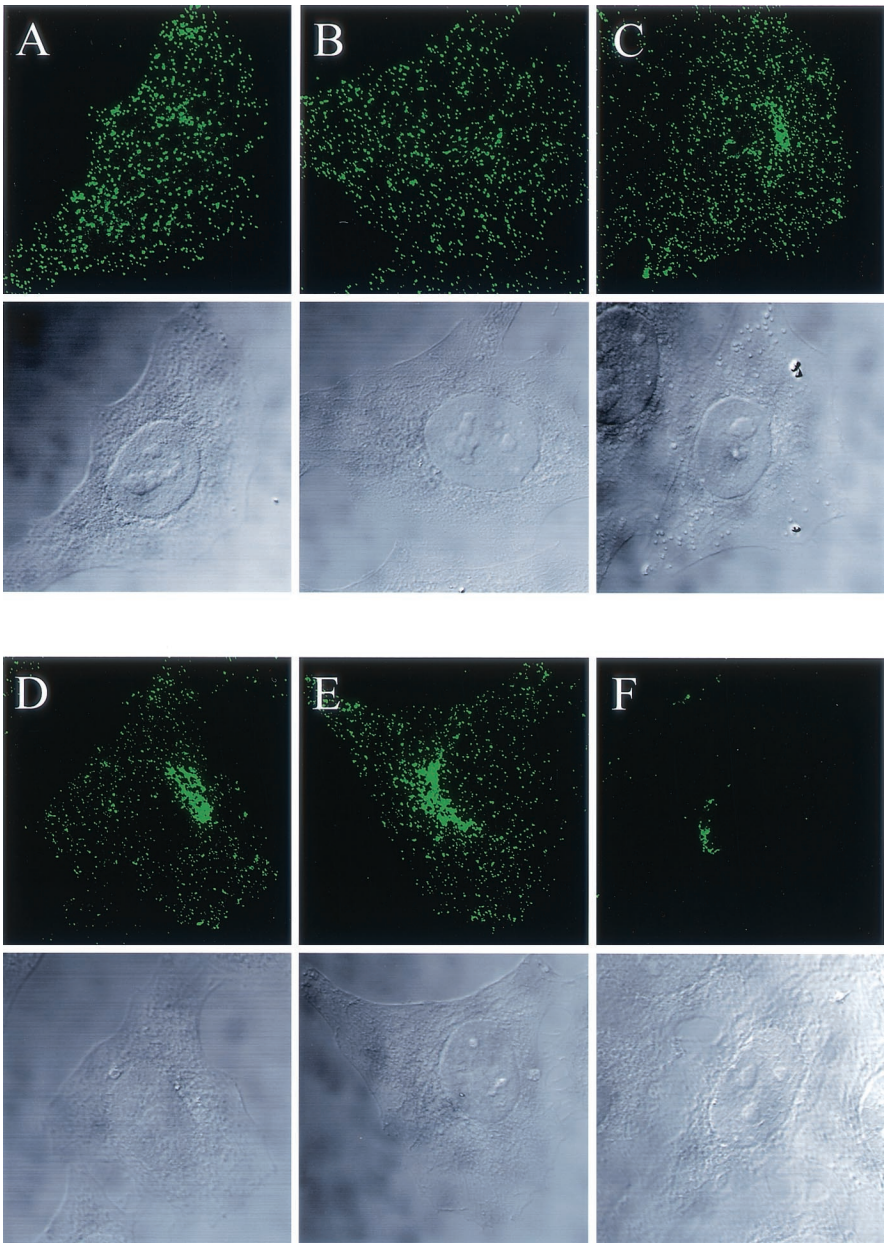

FIG. 4. Time course of infection with TxR-AAV2. HeLa cells were infected at an MOI of 10^4 with TxR-AAV2 and fixed after the times indicated below. The labeled AAV-2 was detected by immunostaining with the A20 primary antibody and Alexa488-labeled anti-mouse secondary antibody. (A) 60 min at 4°C; (B) 15 min at 37°C; (C) 30 min at 37°C; (D) 60 min at 37°C; (E) 2.5 h at 37°C; (F) 23 h at 37°C. Whole-cell projections of laser scanning confocal microscopy sections are shown. Below each projection, the corresponding transmission light micrograph is shown.

cells were infected with AAV2-CMV-EGFP-WPRE in the presence or absence of bafilomycin A1 (20 nM), and transduction was analyzed 48 or 72 h later by FACS. Whereas the bafilomycin A1-treated HeLa cells showed a considerable (38-fold) drop in transduction efficiency, the reduction in the endothelial cells was more modest, between 2- and 4-fold (Fig. 3). Interestingly, the decrease in transduction efficiency by bafilomycin A1 in the glioma cell line LN-229 was only 1.5-fold, despite the fact that this cell line is highly permissive for AAV-2 transduction, and thus, AAV-2 would be expected to follow the same endosomal pathway as in HeLa cells. Even higher concentrations of bafilomycin A1 (50 and 100 nM), which almost completely abolished transduction in HeLa cells, only reduced transduction a maximum of sevenfold in LN-229 cells (not shown).

Use of fluorescence labeling and antibody detection to visualize the intracellular routing of AAV-2 in different cell types. To allow visualization of the AAV-2 endosomal pathway, a highly purified virus preparation (2×10^{12}/ml) was labeled with Texas Red. Previous studies using fluorescent-dye labeling have shown that in the case of AAV, the labeling incorporates only one or two dye molecules per virus particle (2). Therefore, very high MOIs have to be used for the infections in order to detect the labeled AAV by conventional fluores-

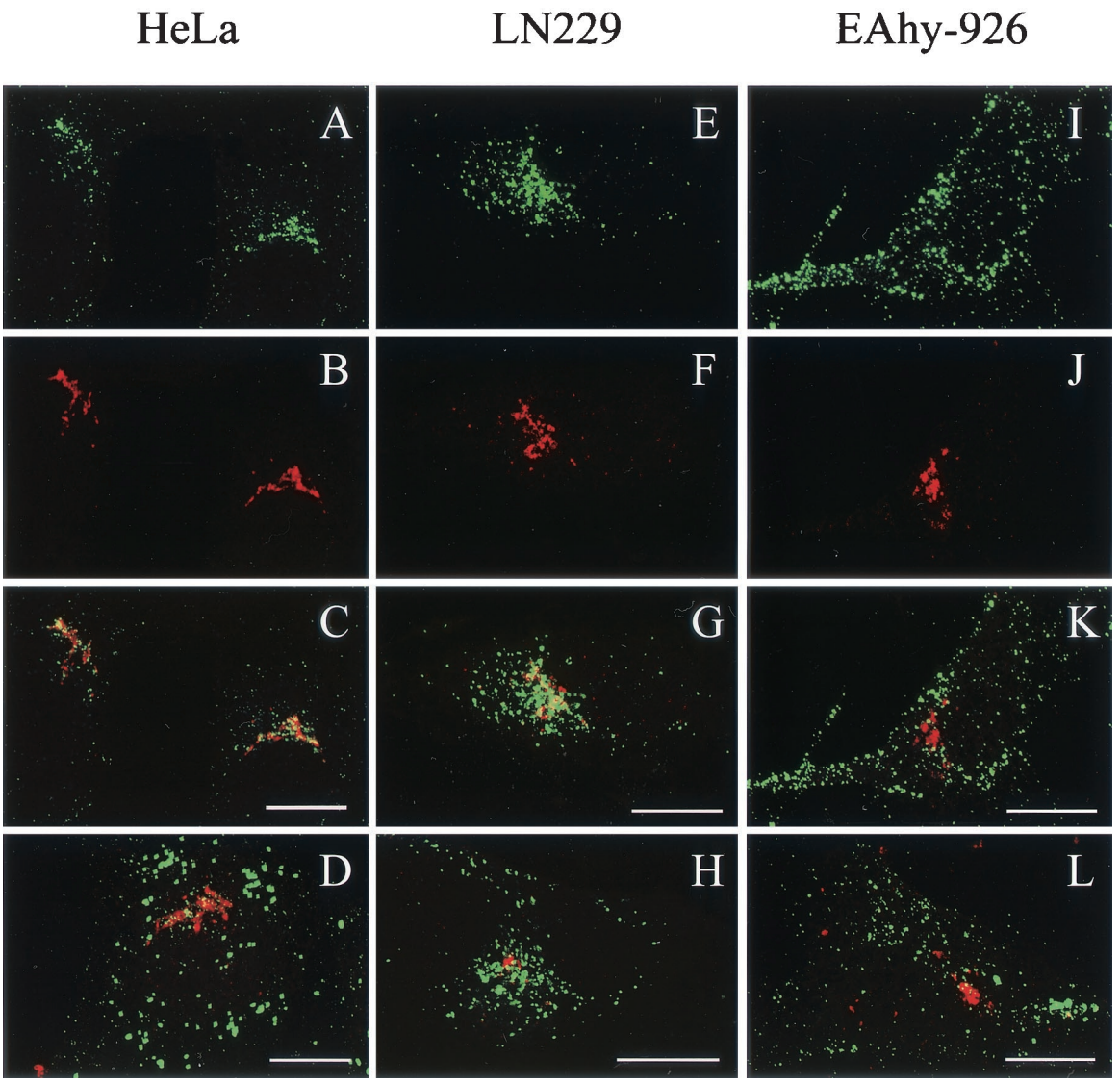

FIG. 5. Infection (2.5 h) with TxR-AAV2 and colocalization with *trans*-Golgi marker in HeLa (A to D), LN-229 (E to H), and EAhy-926 (I to L) cells. The double immunofluorescence staining of TxR-AAV2 (A, E, and I) and galT (B, F, and J) and the overlay (C, G, and K), as well as infections in the presence of bafilomycin A1 and double staining of TxR-AAV2 and galT (D, H, and L), are shown in laser scanning confocal microscopy sections. Bars = 10 μm.

cence microscopy, and this creates a potential risk of aggregate formation of the labeled virus. Alternatively, low-MOI infections may be visualized by single-molecule imaging techniques, as demonstrated recently (28). To be able to use more-physiological MOIs of AAV-2 in the present study, we diluted the Texas Red-labeled stock 50-fold, which resulted in an MOI of 10^4 (particles/cell). Since this MOI of labeled AAV-2 is not readily detectable, due to the reasons mentioned above, the signal was enhanced by an additional antibody detection with the AAV-2 antibody, which recognizes the assembled A20 particle. Figure 4 shows the time course of infection by TxR-AAV2 in HeLa cells. After 1 h of binding at 4°C, the virus was evenly distributed on the cell surface. Fifteen minutes after internalization at 37°C, the labeled AAV-2 was evenly spread in the cytoplasm in structures most likely representing early endosomes and small endosomal transport vesicles (14). Thirty minutes after the start of the infection, the virus started to position itself around the nucleus, and at 1 and 2.5 h postinfection, the bulk of the labeled AAV-2 had accumulated in this perinuclear region. The perinuclear localization of AAV-2 was very stable, as the virus was still detected exclusively in this area 23 h after infection (Fig. 4F). The infectious ability of TxR-AAV2 was demonstrated by EGFP expression in HeLa cells and was shown to be comparable to that of unlabeled AAV-2 (not shown). In addition, experiments performed with unlabeled recombinant AAV-2 showed identical transport kinetics for the virus (not shown).

Next, we wanted to compare the TxR-AAV2 infections in the cell lines that were used for the expression studies (see above). TxR-AAV2 was used to infect EAhy-926, LN-229, and HeLa cells, and the infections were analyzed with a laser scanning confocal microscope at the 2.5-h time point. Figure 5

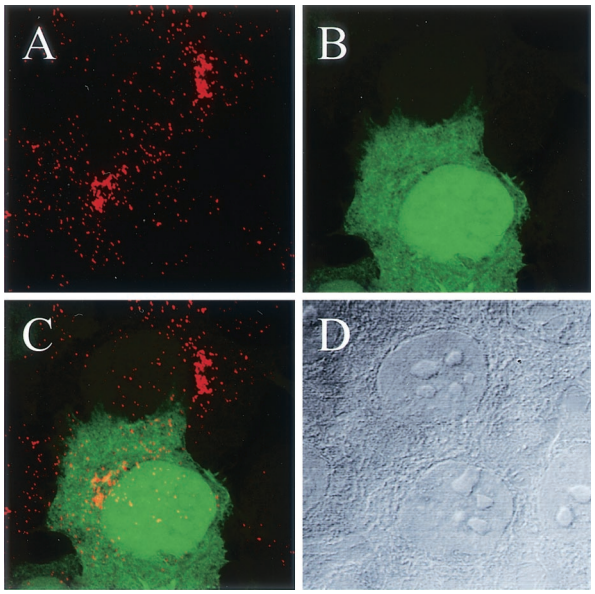

FIG. 6. Golgi localization of AAV-2 does not correlate with transgene expression. (A) HeLa cells were infected with AAV2-CMV-EGFP for 23 h, and the localization of the virus was determined by A20 antibody staining. (B) The transgene expression status of the cells was determined by EGFP fluorescence. (C) Overlay showing that in both the EGFP-positive and -negative cells, AAV-2 particles can still be detected in the Golgi region 23 h after infection. (D) Transmission micrograph of the corresponding light field. Laser scanning confocal images are shown.

shows that in EAhy-926 cells, TxR-AAV2 behaved totally differently than in the highly permissive LN-229 and HeLa cells. In EAhy-926 cells, the virus did not accumulate perinuclearly but seemed to remain in larger aggregates (Fig. 5I). In contrast, in both LN-229 and HeLa, the virus accumulated very efficiently in the perinucleus (Fig. 5A and E). The coimmunostaining of TxR-AAV2 and the *trans*-Golgi marker galactosyl transferase (galT) showed significant colocalization, suggesting that in the permissive cell lines LN-229 and HeLa, AAV-2 travels to the Golgi complex on its infection pathway (Fig. 5C and G). This result, which has not been demonstrated with AAV-2 before, is very reminiscent of what was recently reported for AAV-5 (1). In EAhy-926 cells, TxR-AAV2 failed to localize to the Golgi complex, as shown in Fig. 5K. In order to visualize the response to bafilomycin A1 treatment observed earlier in the expression studies, EAhy-926, LN-229, and HeLa cells were infected with TxR-AAV2 in the presence of bafilomycin A1 (20 nM) and the localization was analyzed 2.5 h later. As shown in Fig. 5D, H, and L, TxR-AAV2 behavior in the presence of bafilomycin A1 recapitulated the result of the expression studies. In HeLa cells, the productive cytoplasmic transport of TxR-AAV2 did not proceed, as shown by the failure of the virus to localize to the Golgi area, instead remaining in the cell periphery as large aggregates. In LN-229 cells, on the other hand, the Golgi localizations of TxR-AAV2 were indistinguishable in the presence or absence of bafilomycin A1. Furthermore, in EAhy-926 cells, bafilomycin A1 did not have an effect on TxR-AAV2 localization, which failed to target the Golgi complex under both conditions. To control the proper functioning of bafilomycin A1 in LN-229 and EAhy-926 cells, acridine orange and FITC-dextran transport experiments were carried out; they showed that bafilomycin A1 function in those cells was comparable to that in HeLa cells (data not shown). In an effort to clarify the significance of the Golgi complex targeting for the AAV-2 transduction process, we infected HeLa cells with AAV2-CMV-EGFP and analyzed both the localization of the virus and the EGFP expression status 23 h later. Surprisingly, there was no correlation between the start of transgene expression and the localization of the virus, as some of the cells continued to retain the virus in the Golgi area although already expressing EGFP (Fig. 6). Hence, this result suggests that a minor AAV-2 population proceeding to the nucleus is sufficient for the start of transgene expression, while a majority of the internalized virus remains in the perinuclear region.

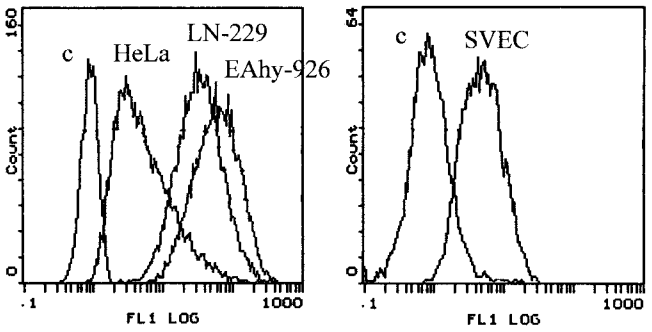

FIG. 7. Analysis of cell surface HSPG expression. The indicated cells in suspension were stained with anti-HS-FITC and analyzed by FACS. c, control cells without antibody treatment.

The expression patterns of HSPGs vary drastically in different cell types. HSPG—more specifically, the HS moiety—has been shown to act as the primary attachment receptor for AAV-2, and in some cell types, the lack of HSPG expression prevents transduction (32). To find out whether a lack of primary receptor is the reason behind the poor transducibility of endothelial cells by AAV-2, we analyzed the expression of HSPGs on the cell types under study with an anti-HS antibody. This antibody recognizes an HS epitope present in most HSPGs and thus allows the detection of a whole variety of different HSPGs. First, the amount of cell surface HSPGs was analyzed by flow cytometry after an anti-HS antibody incubation with the cells in suspension. FACS analysis showed abundant HSPG expression on EAhy-926 and LN-229 cells but only modest expression levels on HeLa cells and SVEC (Fig. 7). This low level of HSPG expression is obviously still enough for the robust AAV-2 transduction seen in HeLa cells. The low level of expression on SVEC, however, was rather surprising, as many essential functions of endothelial cells are known to involve HSPGs (18). Therefore, we also studied HSPG expression with the same antibody on the cells when adherent to their matrix. Figure 8 shows the diversity of the HSPG patterns on the different cell types. In the case of HeLa, LN-229, and EAhy-926 cells, the overall amount of HSPG correlated with the FACS result, although the patterns were variable. In particular, in addition to the robust cell surface expression in EAhy-926 cells, a specific dotty signal was detected on the matrix of these cells. This contrasted with the matrices of HeLa

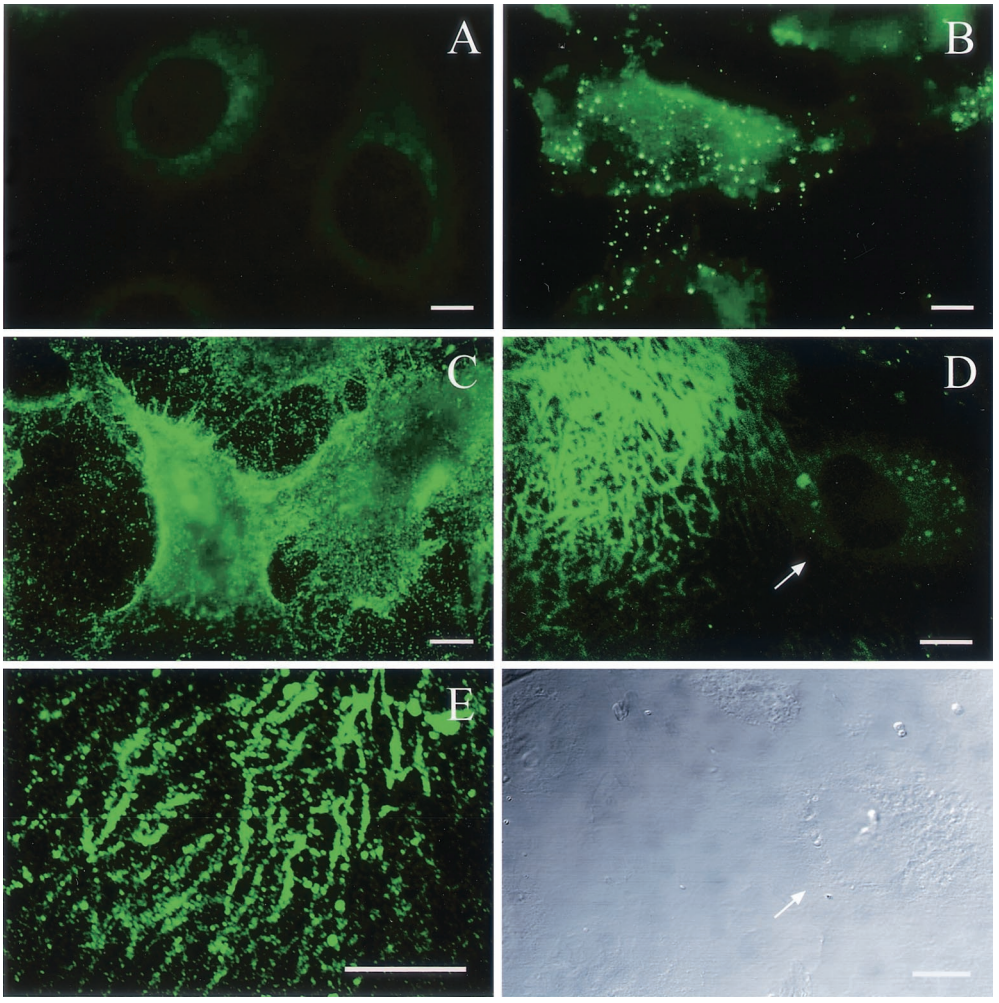

FIG. 8. Analysis of HSPG expression patterns on cultured cells. Immunofluorescence staining with anti-HS-FITC of adherent HeLa cells (A), LN-229 cells (B), EAhy-926 cells (C), and SVEC (D) is shown. The arrow in panel D points to the cell, which shows a remarkably lower level of HSPG expression in comparison to the HSPG deposited on the ECM. Below panel D is the transmission micrograph of the corresponding light field. (E) SVEC infection with AAV2-CMV-EGFP and staining with A20 showing the ECM of SVEC. Bars = 10 μm

and LN-229 cells, which showed no anti-HS staining. In the case of SVEC, the pattern was again totally different. Whereas very weak signals were detected on the cells, the matrix of SVEC showed a massive network of HSPG expression (Fig. 8D). Furthermore, when infected with rAAV2 and stained for the virus, the specific binding pattern showed a similar network-like pattern on the matrix of SVEC (Fig. 8E). Analysis of HSPG expression in mouse skeletal muscle vasculature showed very high expression levels in the abluminal lamina and SMC layers, which are rich in matrix components (Fig. 9). The coimmunostaining of endothelial cells of the muscle sections revealed distinct localization of the endothelium in respect to the underlying HSPG-rich structures. The results described above suggest that on endothelial cells, AAV-2 may bind to the abundant extracellular matrix (ECM) instead of the cell surface, which thus contributes to the low efficiency of transduction of those cells by AAV-2. To functionally test this hypothesis, we infected primary human SVEC both adherent to the matrix and in suspension. The transduction of the endothelial cells in suspension indeed showed 11-fold-higher efficiency than that of the cells attached to the substrate, thus supporting our findings that matrix-bound HSPGs are an important factor regulating AAV-2 transduction (Fig. 10).

DISCUSSION

Recent studies of AAVs have shown that despite their broad host cell spectrum, the efficiency of transduction in different cell types may be highly variable. In practice, this means that for in vivo applications involving less highly transducible cell types, very high MOIs should be used for successful transduction, and this may not be feasible with the present AAV production methods. Factors that limit AAV transduction may exist at all levels of the transduction pathway preceding viral gene expression: cell surface binding, endocytosis, transport in the cytoplasm, and finally, the nuclear events which result in the conversion of the single-stranded AAV genome. Several cytoplasmic determinants that restrict AAV transduction in certain cell types have been identified, and also, different serotypes that more efficiently transduce cells based on their

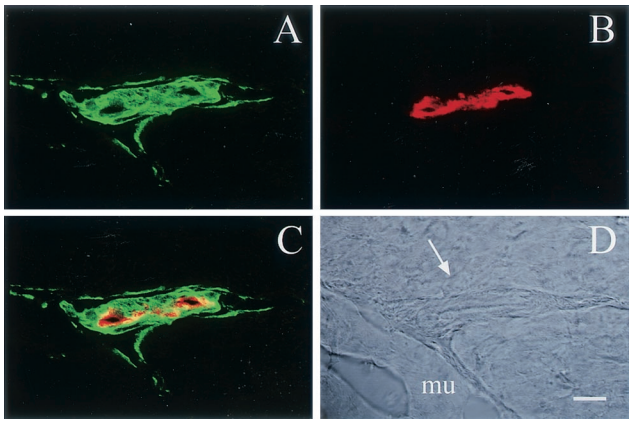

FIG. 9. HSPG expression in mouse skeletal muscle vasculature. Frozen cross sections (10 μm) of mouse gastrocnemius muscle were coimmunostained for HSPGs and endothelium in order to analyze their respective localizations. Laser scanning confocal micrographs are shown. (A) Anti-HS-FITC; (B) anti-CD31; (C) overlay; (D) light field; the arrow points to the lumen of the artery between the muscle fibers (mu). Bar = 10 μm

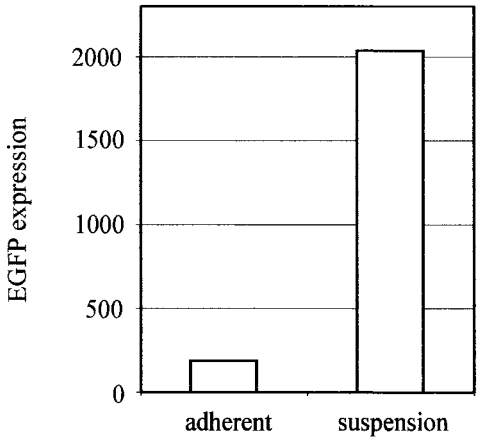

FIG. 10. AAV-2 transduction is enhanced in human primary endothelial cells in suspension. SVEC, either adherent on the matrix or in suspension, were infected with AAV2-CMV-EGFP (MOI = 1,000) for 1 h. After a further 70 h of cultivation, the transduction efficiency (as EGFP expression) was measured by FACS analysis.

differential receptor usage have been uncovered (9, 15, 37). We wanted to study the transducibility of endothelial cells by AAV-2, the most thoroughly characterized AAV serotype. Transduction of endothelial cells would be very useful, for example, for applications linked to cardiovascular gene therapy, and not much is known about the cellular determinants related to AAV-2 transduction in these cells. Studies published so far on the topic show rather variable results regarding the efficiency of transduction, probably reflecting the varied titers or the particular type of application (in vitro versus in vivo) used in the study (4, 11, 22, 25). Our studies show that the transduction efficiency of AAV-2 in endothelial cells is considerably lower than in the highly permissive cell types. The in vivo rabbit carotid artery assay with AAV-2 showed that transduction of medial SMCs was largely preferred to that of intimal endothelial cells, although the virus was applied to the vessel from the luminal side. The SMC transduction in this assay is possible due to the small size of AAV (20 to 25 nm), which allows it to cross the endothelial monolayer, which is not feasible for larger-diameter viruses like retroviruses (27). Thus, despite the poor transduction of endothelial cells in the rabbit carotid artery assay, the ability of AAV-2 to transduce the medial cells efficiently can be beneficial in applications where the expression of angiogenic genes is desired to prevent, e.g., restenosis after bypass surgery (35).

To elucidate the reasons behind the low efficiency of transduction of endothelial cells by AAV-2, we first assayed the effect of proteasome activity on transduction efficiency. In certain poorly transduced cell types, the proteasome is presumed to digest AAV-2 particles that are liberated from the endosomes but have not yet reached the nucleus (7). Another possible role for ubiquitination and proteasome processing of AAV was proposed by Yan et al. (38), who suggested that ubiquitination in some cases may lead to nonproductive rerouting of the virus. That possibility could fit our results on EAhy-926 cells, where AAV-2 routing indeed looked aberrant and proteasome inhibition had a clearly enhancing effect on transduction. The fact that in the primary endothelial cells and in vivo the effect of proteasome inhibition on AAV-2 transduction was modest, if any, may be explained by other inhibitory factors overriding the effect of the proteasome (see below) or simply by the nature of the EAhy-926 cell line, which is a hybrid between HUVEC and the A549 lung carcinoma cell line (10) and therefore expresses the characteristics of both cell types.

With the fluorescently labeled AAV-2, we could confirm the results of the expression studies using bafilomycin A1, where we showed different responses to the inhibition of endosomal acidification in different cell types. Correlating with the dramatic drop in the transduction of HeLa cells after bafilomycin A1 treatment, the labeled AAV-2 together with bafilomycin A1 was very much restrained at the peripheries of these cells. Accordingly, as seen with the endothelial and LN-229 glioma cells by expression analysis, bafilomycin A1 in these cells did not have a significant effect on the transport of the labeled AAV-2. The fact that in LN-229 cells, which are highly permissive for AAV-2, the transduction was not influenced by bafilomycin A1 would suggest that the endosomal pathway of AAV-2 in HeLa cells is not the only one leading to efficient transduction. On the contrary, the phenomenon that was seen only in the permissive cell types, but not in EAhy-926 cells, was AAV-2 targeting of the Golgi complex during transduction. The localization to the Golgi area started to emerge as early as 30 min after the start of infection and was only visible when lower MOIs of the labeled virus, together with antibody detection, were used. With high MOIs of the labeled AAV-2, this phenomenon was not observed, but the virus was seen as larger aggregates which were not advancing efficiently toward the nucleus. The Golgi-like targeting demonstrated here resembles what was recently reported for AAV-5 (1). In the case of AAV-5, abundant staining in the Golgi region was still detected 22 h after the start of infection. Also, here we could demonstrate persistent localization of AAV-2 in the Golgi area as analyzed 23 h after infection. As hypothesized by Bantel-Schaal et al., only a fraction of the Golgi-targeted virus may be

transported into the nucleus, and this is in agreement with the small amount of labeled AAV-2 previously detected in the nucleus (2). However, gene expression by AAV-2 starts as early as 24 h after infection, even in the absence of the helper virus, and thus, the nuclear targeting must proceed rather swiftly to allow sufficient time for the second-strand synthesis of the AAV genome. Indeed, as we show here, transgene expression had already started in some of the cells, despite ongoing prominent Golgi localization of the AAV-2 particles 23 h after infection. In EAhy-926 cells, where the labeled AAV-2 failed to be transported to the Golgi complex, the virus was detected in larger aggregations even with the lower MOI, thus reflecting the aberrant transport. Interestingly, often these aggregates localized deep in either the nuclear or perinuclear area, which may also be the location of proteasomes, shown here to affect AAV-2 transduction in these cells.

Finally, we found significant differences between the expression patterns of the primary receptor of AAV-2 (HSPG) in the cell types under study. In the case of the EAhy-926 endothelial cell line, HSPGs were detected both on the cell surface and in the ECM. However, while the cell surface expression of primary endothelial cells and the endothelium in vivo was shown to be low, the majority of the HSPGs were secreted to the ECM. Furthermore, in the primary endothelial cell cultures, AAV-2 extensively bound to the matrix as well. It is therefore possible that HSPGs in the ECM of endothelial cells compete with the cell surface receptors for AAV-2 binding, which thereby inhibits transduction, and this we could indeed show by demonstrating more efficient transduction of endothelial cells in suspension. The HSPGs expressed by endothelial cells comprise a large and complex family of both cell surface-linked and ECM-associated molecules. In addition to their independent signaling functions, the important endothelial growth factors VEGF and FGF use these molecules as low-affinity coreceptors required for their signaling (6, 21). Therefore, in light of the abundant HSPG expression of endothelial cells, it is not surprising to find that it has a negative impact on AAV-2 transduction. The finding that transduction could be improved by extended viral exposure may be explained by the known storage function and the low binding affinity of HSPGs. Thus, some of the AAV-2 initially bound by the extensive ECM may gradually be released and allowed also to bind to the cell surface receptors.

In conclusion, these experiments have uncovered some of the versatility of the transduction pathways of AAV-2 in different cell types, and the results will help in designing more appropriate and efficient gene transfer protocols for AAV, especially those involving endothelial cells.

ACKNOWLEDGMENTS

We thank Urs Greber and Dmitri Chilov for valuable discussions. Werner Boll is acknowledged for his help with the confocal microscope.

This work was financially supported by The Swiss Cancer League (K.P.), the Academy of Finland (M.G. and S.Y.-H.), and the Swiss National Foundation (H.J., T.F.L., and H.B.).

REFERENCES

1. **Bantel-Schaal, U., B. Hub, and J. Kartenbeck.** 2002. Endocytosis of adeno-associated virus type 5 leads to accumulation of virus particles in the Golgi compartment. J. Virol. **76:**2340–2349.
2. **Bartlett, J. S., R. Wilcher, and R. J. Samulski.** 2000. Infectious entry pathway of adeno-associated virus and adeno-associated virus vectors. J. Virol. **74:**2777–2785.
3. **Berns, K. I., and C. Giraud.** 1996. Biology of adeno-associated virus. Curr. Top. Microbiol. Immunol. **218:**1–23.
4. **Byun, J., J. M. Heard, J. E. Huh, S. J. Park, E. A. Jung, J. O. Jeong, H. C. Gwon, and D. K. Kim.** 2001. Efficient expression of the vascular endothelial growth factor gene in vitro and in vivo, using an adeno-associated virus vector. J. Mol. Cell Cardiol. **33:**295–305.
5. **Chao, H., Y. Liu, J. Rabinowitz, C. Li, R. J. Samulski, and C. E. Walsh.** 2000. Several log increase in therapeutic transgene delivery by distinct adeno-associated viral serotype vectors. Mol. Ther. **2:**619–623.
6. **Cross, M. J., and L. Claesson-Welsh.** 2001. FGF and VEGF function in angiogenesis: signalling pathways, biological responses and therapeutic inhibition. Trends Pharmacol. Sci. **22:**201–207.
7. **Douar, A. M., K. Poulard, D. Stockholm, and O. Danos.** 2001. Intracellular trafficking of adeno-associated virus vectors: routing to the late endosomal compartment and proteasome degradation. J. Virol. **75:**1824–1833.
8. **Duan, D., Q. Li, A. W. Kao, Y. Yue, J. E. Pessin, and J. F. Engelhardt.** 1999. Dynamin is required for recombinant adeno-associated virus type 2 infection. J. Virol. **73:**10371–10376.
9. **Duan, D., Y. Yue, Z. Yan, J. Yang, and J. F. Engelhardt.** 2000. Endosomal processing limits gene transfer to polarized airway epithelia by adeno-associated virus. J. Clin. Investig. **105:**1573–1587.
10. **Edgell, C. J., C. C. McDonald, and J. B. Graham.** 1983. Permanent cell line expressing human factor VIII-related antigen established by hybridization. Proc. Natl. Acad. Sci. USA **80:**3734–3737.
11. **Eslami, M. H., S. P. Gangadharan, X. Sui, K. K. Rhynhart, R. O. Snyder, and M. S. Conte.** 2000. Gene delivery to in situ veins: differential effects of adenovirus and adeno-associated viral vectors. J. Vasc. Surg. **31:**1149–1159.
12. **Greber, U. F., M. Y. Nakano, and M. Suomalainen.** 1998. Adenovirus entry into cells: a quantitative fluorescence approach. Methods Mol. Med. **21:**217–230.
13. **Grimm, D., A. Kern, K. Rittner, and J. A. Kleinschmidt.** 1998. Novel tools for production and purification of recombinant adenoassociated virus vectors. Hum. Gene Ther. **9:**2745–2760.
14. **Gruenberg, J.** 2001. The endocytic pathway: a mosaic of domains. Nat. Rev. Mol. Cell Biol. **2:**721–730.
15. **Halbert, C. L., E. A. Rutledge, J. M. Allen, D. W. Russell, and A. D. Miller.** 2000. Repeat transduction in the mouse lung by using adeno-associated virus vectors with different serotypes. J. Virol. **74:**1524–1532.
16. **Hansen, J., K. Qing, and A. Srivastava.** 2001. Adeno-associated virus type 2-mediated gene transfer: altered endocytic processing enhances transduction efficiency in murine fibroblasts. J. Virol. **75:**4080–4090.
17. **Hansen, J., K. Qing, and A. Srivastava.** 2001. Infection of purified nuclei by adeno-associated virus 2. Mol. Ther. **4:**289–296.
18. **Iozzo, R. V., and J. D. San Antonio.** 2001. Heparan sulfate proteoglycans: heavy hitters in the angiogenesis arena. J. Clin. Investig. **108:**349–355.
19. **Korhonen, J., I. Lahtinen, M. Halmekyto, L. Alhonen, J. Janne, D. Dumont, and K. Alitalo.** 1995. Endothelial-specific gene expression directed by the tie gene promoter in vivo. Blood **86:**1828–1835.
20. **Monahan, P. E., and R. J. Samulski.** 2000. Adeno-associated virus vectors for gene therapy: more pros than cons? Mol. Med. Today **6:**433–440.
21. **Nangia-Makker, P., S. Baccarini, and A. Raz.** 2000. Carbohydrate-recognition and angiogenesis. Cancer Metastasis Rev. **19:**51–57.
22. **Nicklin, S. A., H. Buening, K. L. Dishart, M. de Alwis, A. Girod, U. Hacker, A. J. Thrasher, R. R. Ali, M. Hallek, and A. H. Baker.** 2001. Efficient and selective AAV2-mediated gene transfer directed to human vascular endothelial cells. Mol. Ther. **4:**174–181.
23. **Paterna, J. C., T. Moccetti, A. Mura, J. Feldon, and H. Bueler.** 2000. Influence of promoter and WHV post-transcriptional regulatory element on AAV-mediated transgene expression in the rat brain. Gene Ther. **7:**1304–1311.
24. **Qing, K., C. Mah, J. Hansen, S. Zhou, V. Dwarki, and A. Srivastava.** 1999. Human fibroblast growth factor receptor 1 is a co-receptor for infection by adeno-associated virus 2. Nat. Med. **5:**71–77.
25. **Richter, M., A. Iwata, J. Nyhuis, Y. Nitta, A. D. Miller, C. L. Halbert, and M. D. Allen.** 2000. Adeno-associated virus vector transduction of vascular smooth muscle cells in vivo. Physiol. Genomics **2:**117–127.
26. **Rivett, A. J.** 1998. Intracellular distribution of proteasomes. Curr. Opin. Immunol. **10:**110–114.
27. **Rome, J. J., V. Shayani, M. Y. Flugelman, K. D. Newman, A. Farb, R. Virmani, and D. A. Dichek.** 1994. Anatomic barriers influence the distribution of in vivo gene transfer into the arterial wall. Modeling with microscopic tracer particles and verification with a recombinant adenoviral vector. Arterioscler. Thromb. **14:**148–161.
28. **Seisenberger, G., M. U. Ried, T. Endress, H. Buning, M. Hallek, and C. Brauchle.** 2001. Real-time single-molecule imaging of the infection pathway of an adeno-associated virus. Science **294:**1929–1932.
29. **Smith-Arica, J. R., and J. S. Bartlett.** 2001. Gene therapy: recombinant adeno-associated virus vectors. Curr. Cardiol. Rep. **3:**43–49.
30. **Stupack, D. G., and D. A. Cheresh.** 2002. ECM remodeling regulates angiogenesis: endothelial integrins look for new ligands. Sci. STKE **119:**E7.

31. **Summerford, C., J. S. Bartlett, and R. J. Samulski.** 1999. αVβ5 integrin: a co-receptor for adeno-associated virus type 2 infection. Nat. Med. **5:**78–82.
32. **Summerford, C., and R. J. Samulski.** 1998. Membrane-associated heparan sulfate proteoglycan is a receptor for adeno-associated virus type 2 virions. J. Virol. **72:**1438–1445.
33. **Teramoto, S., T. Ishii, T. Matsuse, and Y. Fukuchi.** 2000. Recombinant adeno-associated virus vectors efficiently transduce foreign genes into bovine aortic endothelial cells: comparison with adenovirus vectors. Jpn. J. Pharmacol. **84:**206–212.
34. **Tsou, R., and F. F. Isik.** 2001. Integrin activation is required for VEGF and FGF receptor protein presence on human microvascular endothelial cells. Mol. Cell Biochem. **224:**81–89.
35. **Turunen, M. P., M. O. Hiltunen, and S. Yla-Herttuala.** 1999. Gene therapy for angiogenesis, restenosis and related diseases. Exp. Gerontol. **34:**567–574.
36. **Van Meir, E., Y. Sawamura, A. C. Diserens, M. F. Hamou, and N. de Tribolet.** 1990. Human glioblastoma cells release interleukin 6 in vivo and in vitro. Cancer Res. **50:**6683–6688.
37. **Walters, R. W., S. M. Yi, S. Keshavjee, K. E. Brown, M. J. Welsh, J. A. Chiorini, and J. Zabner.** 2001. Binding of adeno-associated virus type 5 to 2,3-linked sialic acid is required for gene transfer. J. Biol. Chem. **276:**20610–20616.
38. **Yan, Z., R. Zak, G. W. Luxton, T. C. Ritchie, U. Bantel-Schaal, and J. F. Engelhardt.** 2002. Ubiquitination of both adeno-associated virus type 2 and 5 capsid proteins affects the transduction efficiency of recombinant vectors. J. Virol. **76:**2043–2053.
39. **Yang, Z., F. Ruschitzka, T. J. Rabelink, G. Noll, F. Julmy, H. Joch, V. Gafner, I. Aleksic, U. Althaus, and T. F. Luscher.** 1997. Different effects of thrombin receptor activation on endothelium and smooth muscle cells of human coronary bypass vessels. Implications for venous bypass graft failure. Circulation **95:**1870–1876.
40. **Yla-Herttuala, S., J. Luoma, H. Viita, T. Hiltunen, T. Sisto, and T. Nikkari.** 1995. Transfer of 15-lipoxygenase gene into rabbit iliac arteries results in the appearance of oxidation-specific lipid-protein adducts characteristic of oxidized low density lipoprotein. J. Clin. Investig. **95:**2692–2698.
41. **Zolotukhin, S., B. J. Byrne, E. Mason, I. Zolotukhin, M. Potter, K. Chesnut, C. Summerford, R. J. Samulski, and N. Muzyczka.** 1999. Recombinant adeno-associated virus purification using novel methods improves infectious titer and yield. Gene Ther. **6:**973–985.